

Published in final edited form as:

Nature. 2015 October 15; 526(7573): 443–447. doi:10.1038/nature14864.

## $\eta$ -Secretase processing of APP inhibits neuronal activity in the hippocampus

Michael Willem<sup>1,\*</sup>, Sabina Tahirovic<sup>2</sup>, Marc Aurel Busche<sup>3,4,5</sup>, Saak V. Ovsepiyan<sup>2</sup>, Magda Chafai<sup>6</sup>, Scherazad Kootar<sup>6</sup>, Daniel Hornburg<sup>7</sup>, Lewis D.B. Evans<sup>8</sup>, Steven Moore<sup>8</sup>, Anna Daria<sup>1</sup>, Heike Hampel<sup>1</sup>, Veronika Müller<sup>1</sup>, Camilla Giudici<sup>1</sup>, Brigitte Nuscher<sup>1</sup>, Andrea Wenninger-Weinzierl<sup>2</sup>, Elisabeth Kremmer<sup>2,5,9</sup>, Michael T. Heneka<sup>10,11</sup>, Dietmar R. Thal<sup>12</sup>, Vilmantas Giedraitis<sup>13</sup>, Lars Lannfelt<sup>13</sup>, Ulrike Müller<sup>14</sup>, Frederick J. Livesey<sup>8</sup>, Felix Meissner<sup>7</sup>, Jochen Herms<sup>2</sup>, Arthur Konnerth<sup>4,5</sup>, H el ene Marie<sup>6</sup>, and Christian Haass<sup>1,2,5,\*</sup>

<sup>1</sup>Biomedical Center (BMC), Ludwig-Maximilians-University Munich, 81377 Munich, Germany

<sup>2</sup>German Center for Neurodegenerative Diseases (DZNE) Munich, 81377 Munich, Germany

<sup>3</sup>Department of Psychiatry and Psychotherapy, Technische Universit at M unchen, 81675 Munich, Germany

<sup>4</sup>Institute of Neuroscience, Technische Universit at M unchen, 80802 Munich, Germany

<sup>5</sup>Munich Cluster for Systems Neurology (SyNergy)

<sup>6</sup>Institut de Pharmacologie Mol culaire et Cellulaire (IPMC), Centre National de la Recherche Scientifique (CNRS), Universit e de Nice Sophia Antipolis, UMR 7275, 06560 Valbonne, France

<sup>7</sup>Max Planck Institute of Biochemistry, Martinsried, 82152, Germany

<sup>8</sup>Gurdon Institute, Cambridge Stem Cell Institute & Department of Biochemistry, University of Cambridge, Cambridge CB2 1QN, UK

<sup>9</sup>Institute of Molecular Immunology, German Research Center for Environmental Health, 81377 Munich, Germany

<sup>10</sup>Department of Neurology, Clinical Neuroscience Unit, University of Bonn, 53127 Bonn, Germany

<sup>11</sup>German Center for Neurodegenerative Diseases (DZNE) Bonn, 53175 Bonn, Germany

---

\*To whom correspondence should be addressed: christian.haass@mail03.med.uni-muenchen.de or michael.willem@mail03.med.uni-muenchen.de.

### Author contributions

M.W. and C.H. designed the study and interpreted the results. M.W. generated all biochemical data together with H.H., V.M, B.N. and C.G.. S.T. supported by A.W.-W. provided primary neuronal cultures, performed and analyzed immunohistological stainings and together with A.D. performed LCM. D.R.T. provided and analyzed human brain sections. M.T.H. provided CSF samples. U.M. provided APP KO mice. E.K. produced new monoclonal antibodies. D.H. and F.M. designed and conducted mass spectrometry and data analysis. L.D.B.E, S.M. and F.J.L. carried out BACE1 inhibition of human neurons. H.M. together with M.C. and S.K. performed all electrophysiological recordings (LTP) *in vitro* and analysis in relation to application of peptides. S.V.O. together with J.H. performed all electrophysiological recordings (LTP) *in vitro* in relation to the BACE1 inhibitor tests. M.A.B together with A.K. performed all Ca<sup>2+</sup>-Imaging experiments *in vivo* and analysis. M.W. and C.H. wrote the manuscript with input from the other authors. Correspondence and requests for materials should be addressed to M.W. and C.H.

### Competing financial interests

The authors declare no competing financial interests. A patent is pending.

<sup>12</sup>Institute of Pathology - Laboratory for Neuropathology, University of Ulm, 89081 Ulm, Germany

<sup>13</sup>Department of Public Health/Geriatrics, Uppsala University, Uppsala, Sweden

<sup>14</sup>Institute for Pharmacy and Molecular Biotechnology IPMB, Functional Genomics, University of Heidelberg, 69120 Heidelberg, Germany

## Abstract

Alzheimer's disease (AD) is characterized by the accumulation of amyloid plaques, which are predominantly composed of amyloid  $\beta$ -peptide ( $A\beta$ )<sup>1</sup>. Two principal physiological pathways either prevent or promote  $A\beta$  generation from its precursor (amyloid precursor protein; APP) in a competitive manner<sup>1</sup>. Modulation of the amyloidogenic pathway is currently exploited by anti- $A\beta$  therapeutic strategies<sup>2</sup>. Although APP processing has been studied in great detail, unknown proteolytic events appear to hinder stoichiometric analyses of APP metabolism *in vivo*<sup>3</sup>. We now identified higher molecular weight C-terminal fragments of APP (CTF- $\eta$ ) in addition to the long-known  $\alpha$ - and  $\beta$ -secretase (a disintegrin and metalloproteinase; ADAM10 and  $\beta$ -site APP cleaving enzyme 1; BACE1) generated CTF- $\alpha$  and CTF- $\beta$ . Generation of CTF- $\eta$  is mediated in part by membrane bound matrix-metalloproteinases such as MT5-MMP, referred to as  $\eta$ -secretase activity.  $\eta$ -Secretase cleavage occurs primarily at amino acids 504/505 of APP<sub>695</sub> releasing a truncated, soluble APP ectodomain (sAPP- $\eta$ ). Upon shedding of sAPP- $\eta$  CTF- $\eta$  is further processed by ADAM10 and BACE1 to release long and short  $A\eta$  peptides ( $A\eta$ - $\alpha$  and  $A\eta$ - $\beta$ ).  $A\eta$  peptides are therefore distinct from N-terminally extended  $A\beta$  variants<sup>4,5</sup>, since they do not extend to the  $\gamma$ -secretase cleavage sites.  $\eta$ -Secretase produced CTFs are enriched in dystrophic neurites in an AD mouse model and human AD brains<sup>6</sup>. Genetic and pharmacological inhibition of BACE1 activity results in a robust accumulation of CTF- $\eta$  and  $A\eta$ - $\alpha$ . In mice treated with a potent BACE1 inhibitor hippocampal long-term potentiation (LTP) was reduced. Strikingly, when recombinant or synthetic  $A\eta$ - $\alpha$  was applied on hippocampal slices *ex vivo*, LTP was lowered. Furthermore, *in vivo* single cell two-photon calcium imaging revealed that hippocampal neuronal activity was attenuated by  $A\eta$ - $\alpha$ . These findings not only demonstrate a major physiologically relevant APP processing pathway but may also suggest potential translational relevance for therapeutic strategies targeting APP processing.

## Keywords

Alzheimer's disease; Amyloid  $\beta$ -peptide; APP; BACE1; MMP; Neurodegeneration; Secretase

---

Intensive efforts are on the way to develop therapeutic strategies targeting  $A\beta$ , the major component of the Alzheimer's disease amyloid plaques<sup>1</sup>.  $A\beta$  is generated from APP by proteolytic processing. First,  $\beta$ -secretase, identified as BACE1, cleaves at the Met-Asp bond of the  $A\beta$  domain and generates CTF- $\beta$ , which is further processed to  $A\beta$  by intramembrane cleavage by  $\gamma$ -secretase<sup>7</sup>. Liberated  $A\beta$  forms soluble synaptotoxic oligomers, which are believed to be the major culprits of the disease<sup>1</sup>. Thus targeting the production of synaptotoxic  $A\beta$  species by  $\beta$ -secretase inhibition is a promising therapeutic strategy and clinical studies with high affinity BACE1 inhibitors are currently evaluated<sup>8,9</sup>. Decreasing BACE1 activity leads to an increase of non-amyloidogenic processing of APP by ADAM10<sup>10</sup>. Similarly, enhancing  $\alpha$ -secretase activity reduced  $A\beta$  production and plaque

formation<sup>11</sup>. However, stable isotope labeling kinetics upon *in vivo* inhibition of BACE1 in monkeys revealed 83% decrease of sAPP- $\beta$  with only 35% increase of sAPP- $\alpha$ . Thus, the fate of almost 50% of the initially labeled APP remains unclear. In addition to the two major and well-studied proteolytic processing pathways, APP is also cleaved in minor processing pathways utilizing different proteases<sup>12</sup>. Furthermore, 17-35 kDa N-APP fragments are generated during early development and upon trophic-factor deprivation<sup>13–15</sup>. However, such alternative APP metabolites were not observed to accumulate upon BACE1 inhibition. To identify novel proteolytic pathways of APP we searched for C-terminal fragments (CTFs) different from those giving rise to p3 (CTF- $\alpha$ ) or A $\beta$  (CTF- $\beta$ )<sup>16–18</sup> mouse brains. A novel CTF with an approximate molecular weight of 30 kDa was revealed which was recognized by an antibody to the C-terminus of APP (Y188) and was absent in the brains of APP knockout mice (APP KO)<sup>19</sup> (Fig. 1a; antibodies used are described in supplementary Tab. S1). The molecular weight of the novel CTF suggests an additional physiological cleavage of APP N-terminal to the known cleavage sites of  $\beta$ -, and  $\alpha$ -secretases, which we named accordingly  $\eta$ -cleavage of APP (supplementary Fig. S1). In the soluble fraction we detected the N-terminal cleavage product (sAPP- $\eta$ ; see supplementary Fig. S2), with a molecular weight of approximately 80 kDa that clearly distinguishes it from alternative N-terminal APP fragments described previously<sup>13–15</sup>. In addition, we observed lower molecular weight soluble peptides (A $\eta$ ), which presumably derived from BACE1 (A $\eta$ - $\beta$ ) or ADAM10 (A $\eta$ - $\alpha$ ) mediated processing of CTF- $\eta$  or alternatively from cleavage of sAPP- $\alpha$ / $\beta$  (Fig. 1b). A $\eta$  was identified in the soluble fraction of mouse brains as several closely spaced peptides by antibody M3.2 (Fig. 1b), demonstrating that some of these fragments contain the N-terminal part of the A $\beta$  domain and are most likely ending at the  $\alpha$ -secretase cleavage site. A $\eta$  fragments were further validated by antibody 9478D directed against an epitope N-terminal to the A $\beta$  domain (Fig. 1b).

The presence of endogenous CTF- $\eta$  as well as A $\eta$  in the mouse brain suggests that A $\eta$  generation occurs by a physiological APP processing pathway similar to A $\beta$  production<sup>20,21</sup>. Consistent with physiological  $\eta$ -secretase cleavage of APP in wild type mice, we observed increased CTF- $\eta$  and A $\eta$  production in brain homogenates of APPS1-21 transgenic mice which express the APP Swedish mutation as well as the presenilin 1 L166P mutation<sup>22</sup> (Fig 1c & d). Additionally, antibody 192swe<sup>23</sup> selectively identified the A $\eta$ - $\beta$  species truncated at the BACE1 cleavage site in brain homogenates of APPS1-21 transgenic mice (Fig. 1d). Consistent with the increased BACE1 cleavage of Swedish mutant APP, only minor amounts of A $\eta$ - $\alpha$  were detected in this mouse model with the antibody 2D8 (Fig 1d). Physiological  $\eta$ -secretase processing was further confirmed in cerebrospinal fluid (CSF) from humans with and without the Swedish mutation (APPswe)<sup>24</sup> (Fig. 1e). Using antibody 192swe A $\eta$ - $\beta$  was selectively detected in CSF of patients with the Swedish mutation, whereas antibody 2D8 detected A $\eta$ - $\alpha$  in all analyzed samples (Fig. 1e). Thus A $\eta$ - $\alpha$  and A $\eta$ - $\beta$  are both produced under physiological conditions in humans. Moreover, while these peptides are generated by  $\eta$ -secretase cleavage N-terminal to the A $\beta$ -domain, they do not reach the  $\gamma$ -secretase site (see also mass spectrometric analysis in Fig. 1f), demonstrating that they are different to the previously described N-terminally extended A $\beta$  variants<sup>4,5</sup>.

Membrane bound matrix-metalloproteinases like MT1-MMP and MT5-MMP were shown to cleave APP *in vitro* at a site consistent with the molecular weight of  $\eta$ -secretase processing products<sup>25,26</sup>. We therefore produced a neo-epitope specific antibody (10A8; supplementary Fig. S2), to identify the  $\eta$ -secretase cleavage site. Antibody 10A8 detected a protein corresponding to sAPP- $\eta$  with an approximate molecular weight of 80 kDa in mouse brain lysates, which is absent in the APPKO brain (supplementary Fig. S2). Of note, antibody 10A8 failed to detect sAPP- $\alpha/\beta$  (supplementary Fig. S2), confirming its selectivity for the  $\eta$ -cleavage site. Thus  $\eta$ -secretase cleavage of APP may occur *in vivo* at least in part at amino acids 504/505 of APP<sub>695</sub>. To finally elucidate the N- and C- terminal cleavage sites of A $\eta$  peptides, we performed immunoprecipitation with antibodies 9476, 9480, 2D8 and 2E9 (supplementary Fig S3 a and b). Isolated A $\eta$  peptides were digested with three different proteases to produce multiple overlapping peptides and analyzed by high-resolution Quadrupole Orbitrap mass spectrometry<sup>27</sup>. We identified multiple peptides covering the entire sequence between the cleavage site N(504)/M(505) of APP<sub>695</sub> starting with the sequence MISEPRISY after the  $\eta$ -secretase cleavage site (Fig. 1f). Mass spectrometry also supports the C-terminal cleavages at the  $\beta$ - and  $\alpha$ -secretase sites. Following immunoprecipitation with 2D8 N-terminal extended peptides similar to those described by Portelius et al.<sup>4</sup> were also observed besides the novel A $\eta$  peptides (Fig. 1f and supplementary Fig. S3c).

As the above-described identification of a major  $\eta$ -secretase cleavage site at amino acid 505 of APP is consistent with the previously described *in vitro* cleavage sites of APP by MT1-MMP and MT5-MMP<sup>25,26</sup>, we investigated brains from MT5- and MT1-MMP KO mice (supplementary Fig. S4)<sup>28,29</sup>. Whereas a knockout of MT1-MMP had no significant effect on A $\eta$ - $\alpha$  levels (supplementary Fig. S4c), the generation of A $\eta$ - $\alpha$  was somewhat reduced in brains from MT5-MMP KO mice (supplementary Fig. S4b). Furthermore, upon overexpression of MT-5 MMP in murine N2a cells, a selective increase in A $\eta$ - $\alpha$  peptide of approximately 16 kDa was observed (data not shown). Thus, MT5-MMP displays  $\eta$ -secretase activity in intact mouse brains although contribution of additional  $\eta$ -secretases must be considered.

While investigating protease inhibitors capable of blocking  $\eta$ -secretase, we observed that pharmacological BACE1 inhibition led to a pronounced accumulation of the long A $\eta$ - $\alpha$  species in CHO 7PA2 cells (Fig. 2a). This indicates that upon blockade of  $\beta$ -secretase activity, processing by  $\alpha$ -secretase leads to enhanced production of the long A $\eta$ - $\alpha$  species to the expense of shorter BACE1 generated A $\eta$ - $\beta$ . Similarly, BACE1 inhibition also led to an accumulation of endogenous CTF- $\eta$  and enhanced production of endogenous A $\eta$ - $\alpha$  in primary mouse hippocampal neurons (Fig. 2b-c) as well as human neurons differentiated from embryonic pluripotent stem cells (hEPSC; H930; Fig. 2d-g). Furthermore, in human neurons we not only detected a 65% increase of the slightly longer A $\eta$ - $\alpha$  species upon BACE inhibition, but also a concomitant decrease of A $\eta$ - $\beta$  peptides (Fig. 2e, upper panel). Importantly  $\eta$ -secretase processing significantly exceeded amyloidogenic processing ( $9,5 \pm 1,87$  times A $\eta$  over A $\beta$  estimated for human neurons;  $p > 0,001$ ; Student's t-test). Pharmacological intervention *in vivo* with a single oral dose of the BACE1 inhibitor RO550888731 caused a significant and time dependent increase of CTF- $\eta$  and A $\eta$ - $\alpha$  in APP<sub>V717I</sub> transgenic mice<sup>32</sup> (Fig. 2h), an effect that was fully reversible presumably due to

clearance of the inhibitor after 24 h of administration. In agreement with this, increased CTF- $\eta$  and A $\eta$ - $\alpha$  was also observed upon genetic ablation of the BACE1 encoding gene *in vivo* 33(Fig. 2i).

To identify a potential contribution of  $\eta$ -secretase processing to AD pathology, immunohistochemical analyses were performed with brains derived from 6 months old APPPS1-2134 mice. This revealed co-labeling of antibody Y188 with antibody 2E9 in dystrophic neurites. No signal for the A $\eta$  domain was obtained in plaque cores where aggregated A $\beta$  was detected by 6E10 staining (supplementary Fig. S5a; similar data were obtained in human AD brains (supplementary Fig. S6)). This suggests that CTF- $\eta$  may accumulate together with full-length APP and CTF- $\alpha\beta$  in dystrophic neurites surrounding neuritic plaques of APPPS1-21 mice. To verify directly the accumulation of CTF- $\eta$  in dystrophic neurites, we used laser capture microdissection (LCM) to differentially enrich for proteins accumulating in dystrophic neurites and plaque cores. Indeed, Western blot analysis revealed not only CTF- $\beta$  and lower levels of CTF- $\alpha$ , but also CTF- $\eta$  within the halo of dystrophic neurites and not within the plaque core area or regions devoid of plaques (supplementary Fig. S5b; upper panel). As expected, A $\beta$  was observed within the plaque core as well as in the surrounding halo (supplementary Fig. S5b; lower panel).

Since cleavage products of A $\eta$  processing of APP accumulate upon BACE1 inhibition (Fig. 2) and are enriched in dystrophic neurites (see supplementary Fig. S5 and Fig. S6), we examined if soluble A $\eta$  peptides interfere with neuronal function, similar to soluble A $\beta$  oligomers<sup>1</sup>. LTP is considered as a synaptic correlate of memory<sup>35</sup> and is widely used as a model for investigating the neurotoxic effects of A $\beta$  oligomers on synaptic function<sup>36–38</sup>. A single oral dose of BACE1 inhibitor SCH168249639 increased the levels of CTF- $\eta$  and the level of A $\eta$ - $\alpha$  was increased by almost twofold in soluble brain extracts prepared from animals 3 h after treatment (Fig. 3a). When hippocampal slices were exposed to the BACE1 inhibitor SCH168249639, a significant reduction of hippocampal LTP was evident (Fig. 3b and 3c). These findings may suggest an involvement of A $\eta$ - $\alpha$  in LTP deficit under acute blockade of  $\beta$ -secretase activity<sup>39</sup>. To directly validate potential effects of A $\eta$  peptides on synaptic transmission and plasticity, we expressed A $\eta$ - $\beta$  and A $\eta$ - $\alpha$  in CHO cells (Fig. 3d). Concentrated conditioned media were further enriched for A $\eta$  by size exclusion chromatography (SEC) and applied to hippocampal slices prior to LTP induction in CA1 pyramidal neurons. Neither A $\eta$ - $\beta$  nor A $\eta$ - $\alpha$  influenced the baseline synaptic transmission (supplementary Fig. S7). Comparison of LTP 60 min after its induction in the presence of A $\eta$ - $\beta$  or A $\eta$ - $\alpha$  with control conditions (Fig. 3e-h) revealed that A $\eta$ - $\alpha$  lowered the LTP to a degree comparable to synthetic A $\beta$ <sub>S26C</sub><sup>38</sup> (supplementary Fig. S8 a and b) while truncated A $\eta$ - $\beta$  had no effect (Fig. 3f and 3h). In support to this observation a synthetic peptide corresponding to the primary sequence of A $\eta$ - $\alpha$  reduced LTP to a similar extent at a concentration of 100 nM (supplementary Fig. S8 c and d).

To examine direct effects of A $\eta$  peptides on neuronal activity within the intact brain *in vivo*, we utilized two-photon calcium imaging at single cell resolution<sup>40,41</sup>. Figure 4a-d illustrates results from experiments in which the activity of neurons in the CA1 pyramidal cell layer was monitored before and after superfusion of the exposed hippocampus<sup>41</sup> with A $\eta$  peptides or the respective control peptides. A $\eta$ - $\alpha$  strongly suppressed the activity of

hippocampal neurons *in vivo*, an effect not observed with recombinant A $\eta$ - $\beta$  or the control peptide (Fig. 4a-d; see also supplementary Fig S9). By using local application of synthetic A $\eta$ - $\alpha$  peptides to hippocampal neurons, we demonstrate that the inhibitory effect of A $\eta$ - $\alpha$  on neurons was readily reversible upon wash-out (Fig. 4e). Figures 4f and 4g summarize the results from all experiments. Taken together, these data establish that, in addition to LTP inhibition *in vitro* (Fig. 3), A $\eta$ - $\alpha$  has major dampening effects on neuronal activity *in vivo*, supporting the relevance of this newly identified APP derived peptide for neuronal function.

A $\beta$  production occurs under physiological conditions by  $\beta$ - and  $\gamma$ -secretase mediated processing of APP<sup>20,21</sup>. Strong genetic evidence led to the formulation of the amyloid cascade hypothesis and subsequently to A $\beta$  directed therapeutic approaches<sup>42</sup>. However, these early investigations already indicated the presence of additional unknown processing pathways. This was recently highlighted by elegant studies in rhesus macaques, which revealed an 83% decrease of sAPP- $\beta$  but only a 35% increase of sAPP- $\alpha$ <sup>3</sup> upon BACE1 inhibition. We have likely identified this pathway and demonstrate that  $\eta$ -secretase processing products even exceed amyloidogenic processing in cultured cells, rat hippocampal neurons, hEPSC derived human neurons, mouse and human brains, as well as human CSF. Similar to A $\beta$  production, the alternative proteolytic processing pathway occurs under physiological conditions but may be altered during AD pathogenesis. In this novel pathway, APP<sub>695</sub> is cleaved at amino acids 504/505. The remaining APP CTF- $\eta$  is then a substrate for  $\alpha$ - or  $\beta$ -secretase cleavage, which liberates soluble A $\eta$ - $\alpha$  or A $\eta$ - $\beta$ . In addition sAPP $\alpha$ / $\beta$  may also serve as a precursor for A $\eta$  generation. Of note, these peptides do not extend to the  $\gamma$ -secretase cleavage site and are therefore distinct from previously described N-terminally extended A $\beta$  species<sup>4,5</sup>. It is important to note that low-n A $\beta$  oligomer preparations from 7PA2 supernatants contain significant amounts of A $\eta$  (data not shown). Thus the previously observed inhibition of LTP with such fractions may also be attributed to the presence of A $\eta$ .

The physiological functions of endogenous A $\eta$  still need to be evaluated, but it is tempting to speculate that it may be involved in modulation of neuronal activity and synaptic plasticity. The reason for the differential bioactivity of recombinant A $\eta$ - $\alpha$  and A $\eta$ - $\beta$  is currently unclear. One may speculate that the longer A $\eta$ - $\alpha$  is more stable probably due to unknown post-translational modifications. This would be consistent with our observation that in contrast to cell produced A $\eta$ - $\beta$ , 100 nM of synthetic A $\eta$ - $\beta$  inhibits LTP (data not shown).

Accumulation of  $\eta$ -secretase<sup>6</sup> and CTF- $\eta$  within dystrophic neurites in close vicinity to neuritic plaques may also support its potential contribution to AD pathology. Obviously, all APP and presenilin familial AD mutations affect A $\beta$  production and aggregation (reviewed by Haass<sup>7</sup>), whereas the Icelandic mutation (APP<sub>A673T</sub>) prevents AD and dementia by moderately reducing the A $\beta$  production<sup>43</sup>. Indeed, the Swedish mutation decreased A $\eta$ - $\alpha$  by strongly enhancing BACE1 mediated APP processing, as shown in APPPS1-21 transgenic mice. However, when considering that A $\beta$  accumulation may stimulate  $\eta$ -secretase activity and eventually disturb neuronal plasticity, increased  $\eta$ -secretase activity near amyloid plaques<sup>6</sup> (see supplementary Fig. S5 and supplementary Fig. S6) is in line with the amyloid-cascade hypothesis and a central pathological role of A $\beta$  in AD. Our

findings should be considered in the context of ongoing clinical trials with BACE1 inhibitors, since accumulation of A $\eta$ - $\alpha$  may dampen neuronal activity and synaptic plasticity. Together with the finding of numerous brain specific substrates of BACE1<sup>44,45</sup> our data therefore imply that therapeutic inhibition of BACE1 activity requires careful titration to prevent unwanted adverse effects at multiple levels<sup>46</sup>.

## Material and methods

### Biochemical methods

Soluble proteins were extracted from brain hemispheres with DEA buffer<sup>47</sup>, membrane proteins were extracted with RIPA buffer or by applying a membrane preparation protocol as described<sup>48</sup>. All Western blot procedures were done essentially as described<sup>49</sup>.

### BACE1 inhibitor treatment *in vivo*

Three-month-old heterozygous female transgenic mice FVB/N x C57Bl/6J expressing APP<sup>V717I</sup><sup>32</sup> were used for BACE1 inhibition studies. Gavage mediated administration of BACE1 inhibitor RO5508887 (90 mg/kg, 14.06 ml/kg) or vehicle (14.06 ml/kg) was performed once<sup>50</sup>.

### Slice preparation and electrophysiological recordings

OPTIMEM was used to collect CHO cell supernatants. SEC was performed with concentrated CHO supernatants using a FPLC (ÄKTA purifier) equipped with a Superdex<sup>75</sup> column (GE Healthcare). 1 ml samples were collected with a mobile phase flow rate set at 0.5 ml/min in standard ACSF. Acute hippocampal slices were prepared from Swiss mice (PND20-30) and kept in ACSF<sup>51</sup>. Extracellular field excitatory post-synaptic potentials (fEPSPs) were obtained from CA1 pyramidal neurons. After 15-20 minutes of bath application of SEC fractions<sup>52</sup>, LTP was induced by high frequency stimulation. LTP was recorded for 45-60 minutes and statistical analysis was performed on the last 15-20 minutes of recording compared to the baseline fEPSP values.

### *In vivo* two-photon calcium imaging

Two-photon calcium imaging was carried out as described previously<sup>41</sup>. To obtain access to the hippocampus, we carefully removed cortical tissue covering the CA1 region<sup>41,53–55</sup>. The exposed CA1 region was stained with the calcium indicator fluo-8 AM (0.6 mM) using the multi-cell bolus loading technique<sup>56</sup>. Imaging was performed with a custom-built two-photon microscope equipped with a Ti:sapphire laser system. To assess the effects of A $\eta$  peptides on neuronal activity *in vivo*, the peptides or the respective controls were added to the normal Ringer's solution used for perfusion of the recording chamber (bath-application technique; 45 to 60 min each wash-in). In a subset of experiments, synthetic A $\eta$ - $\alpha$  was applied locally by gentle pressure injection through a glass pipette that was placed close to the neurons of interest (local application technique; 40 s each pressure injection).

## Supplementary Material

Refer to Web version on PubMed Central for supplementary material.

## Acknowledgement

The authors thank Dr. Sven Lammich and Dr. Harald Steiner for critical comments. We thank Alice Sülzen, Nagore Astola, Stephanie Diederich, Eric Griebinger and Julia Gobbert for excellent technical help. The APPPS1-21 colony was established from a breeding pair kindly provided by Dr. Mathias Jucker (Hertie Institute University of Tübingen and DZNE-Tübingen). MT1-MMP<sup>-/-</sup> mouse brains were gratefully obtained from Dr. Zhongjun Zhou (University of Hong Kong). MT5-MMP<sup>-/-</sup> mouse brains were gratefully obtained from Dr. Isabel Farinas (University of Valencia, Spain). We thank Dr. Helmut Jacobsen (Hoffmann-La Roche Pharma Research & Early Development, DTA Neuroscience, Basel, Switzerland) for the BACE1 inhibitor RO5508887. This work was supported by the European Research Council under the European Union's Seventh Framework Program (FP7/2007–2013)/ERC Grant Agreement No. 321366-Amyloid (advanced grant to C.H.). The work of D.R.T. was supported by AFI (Grant #13803). The research leading to these results has received funding (F.M., D.H.) from the European Research Council under the European Union's Seventh Framework Programme (FP7/2007-2013) / ERC grant agreement No. 318987 [TOPAG]. We also acknowledge support by grants from Deutsche Forschungsgemeinschaft (MU 1457/9-1, 9-2 to U.M.) and the ERA-Net Neuron (01EW1305A to U.M.). Further support came from the ATIP/AVENIR program (Centre national de la recherche scientifique -CNRS) to H.M.; the French Fondation pour la Coopération Scientifique – Plan Alzheimer (Senior Innovative Grant 2010) to M.C. and H.M. and the French Government (National Research Agency, ANR) through the "Investments for the Future" LABEX SIGNALIFE: program reference #ANR-11-LABX-0028-01 to S.K.. M.A.B was supported by the Langmatz Stiftung. F.J.L. is a Wellcome Trust Investigator. In vivo BACE1 inhibition experiment with APP transgenic mice were performed together with reMYND (Bio-Incubator, 3001 Leuven-Heverlee, Belgium).

## Abbreviations

<b>AD</b>	Alzheimer's disease
<b>ADAM</b>	a disintegrin and metalloproteinase
<b>APP</b>	amyloid precursor protein
<b>A<math>\beta</math></b>	Amyloid $\beta$ -peptide
<b>BACE1</b>	beta-site APP cleaving enzyme 1
<b>CSF</b>	cerebrospinal fluid
<b>CTF</b>	C-terminal fragment
<b>A<math>\eta</math></b>	$\eta$ -secretase cleavage product of APP
<b><math>\eta</math>-secretase</b>	eta-site APP cleaving enzyme
<b>MMP</b>	matrix metalloproteinase
<b>fEPSPs</b>	field excitatory post-synaptic potentials
<b>LCM</b>	laser capture micro-dissection
<b>LTP</b>	long-term potentiation

## References

1. Haass C, Selkoe DJ. Soluble protein oligomers in neurodegeneration: lessons from the Alzheimer's amyloid beta-peptide. *Nat Rev Mol Cell Biol.* 2007; 8:101–112. [PubMed: 17245412]
2. Nygaard HB. Current and Emerging Therapies for Alzheimer's Disease. *Clin Ther.* 2013; 35:1480–1489. [PubMed: 24139420]
3. Dobrowolska JA, et al. CNS amyloid-beta, soluble APP-alpha and -beta kinetics during BACE inhibition. *J Neurosci.* 2014; 34:8336–8346. [PubMed: 24920637]



4. Portelius E, et al. Mass spectrometric characterization of amyloid-beta species in the 7PA2 cell model of Alzheimer's disease. *J Alzheimers Dis.* 2013; 33:85–93. [PubMed: 22886024]
5. Welzel AT, et al. Secreted amyloid beta-proteins in a cell culture model include N-terminally extended peptides that impair synaptic plasticity. *Biochemistry (Mosc).* 2014; 53:3908–3921.
6. Sekine-Aizawa Y, et al. Matrix metalloproteinase (MMP) system in brain: identification and characterization of brain-specific MMP highly expressed in cerebellum. *Eur J Neurosci.* 2001; 13:935–948. [PubMed: 11264666]
7. Haass C. Take five--BACE and the gamma-secretase quartet conduct Alzheimer's amyloid beta-peptide generation. *EMBO J.* 2004; 23:483–488. [PubMed: 14749724]
8. Willem M, Lammich S, Haass C. Function, regulation and therapeutic properties of beta-secretase (BACE1). *Semin Cell Dev Biol.* 2009; 20:175–182. [PubMed: 19429494]
9. Yan R, Vassar R. Targeting the beta secretase BACE1 for Alzheimer's disease therapy. *Lancet Neurol.* 2014; 13:319–329. [PubMed: 24556009]
10. McConlogue L, et al. Partial reduction of BACE1 has dramatic effects on Alzheimer plaque and synaptic pathology in APP Transgenic Mice. *J Biol Chem.* 2007; 282:26326–26334. [PubMed: 17616527]
11. Postina R, et al. A disintegrin-metalloproteinase prevents amyloid plaque formation and hippocampal defects in an Alzheimer disease mouse model. *J Clin Invest.* 2004; 113:1456–1464. [PubMed: 15146243]
12. Simons M, et al. Amyloidogenic processing of the human amyloid precursor protein in primary cultures of rat hippocampal neurons. *J Neurosci.* 1996; 16:899–908. [PubMed: 8558258]
13. Nikolaev A, McLaughlin T, O'Leary DD, Tessier-Lavigne M. APP binds DR6 to trigger axon pruning and neuron death via distinct caspases. *Nature.* 2009; 457:981–989. [PubMed: 19225519]
14. Jefferson T, et al. Metalloprotease meprin beta generates nontoxic N-terminal amyloid precursor protein fragments in vivo. *J Biol Chem.* 2011; 286:27741–27750. [PubMed: 21646356]
15. Vella LJ, Cappai R. Identification of a novel amyloid precursor protein processing pathway that generates secreted N-terminal fragments. *FASEB J.* 2012
16. Haass C, Koo EH, Mellon A, Hung AY, Selkoe DJ. Targeting of cell-surface beta-amyloid precursor protein to lysosomes: alternative processing into amyloid-bearing fragments. *Nature.* 1992; 357:500–503. [PubMed: 1608449]
17. Estus S, et al. Potentially amyloidogenic, carboxyl-terminal derivatives of the amyloid protein precursor. *Science.* 1992; 255:726–728. [PubMed: 1738846]
18. Haass C, et al. b-Amyloid peptide and a 3-kDa fragment are derived by distinct cellular mechanisms. *J Biol Chem.* 1993; 268:3021–3024. [PubMed: 8428976]
19. Muller U, et al. Behavioral and Anatomical Deficits in Mice Homozygous for a Modified Beta-Amyloid Precursor Protein Gene. *Cell.* 1994; 79:755–765. [PubMed: 8001115]
20. Haass C, et al. Amyloid beta-peptide is produced by cultured cells during normal metabolism. *Nature.* 1992; 359:322–325. [PubMed: 1383826]
21. Golde TE, Estus S, Younkin LH, Selkoe DJ, Younkin SG. Processing of the amyloid protein precursor to potentially amyloidogenic derivatives. *Science.* 1992; 255:728–730. [PubMed: 1738847]
22. Radde R, et al. Abeta42-driven cerebral amyloidosis in transgenic mice reveals early and robust pathology. *EMBO Rep.* 2006; 7:940–946. [PubMed: 16906128]
23. Haass C, et al. The Swedish Mutation Causes Early-Onset Alzheimers-Disease by Beta-Secretase Cleavage within the Secretory Pathway. *Nat Med.* 1995; 1:1291–1296. [PubMed: 7489411]
24. Lannfelt L, et al. Amyloid beta-peptide in cerebrospinal fluid in individuals with the Swedish Alzheimer amyloid precursor protein mutation. *Neurosci Lett.* 1995; 199:203–206. [PubMed: 8577398]
25. Higashi S, Miyazaki K. Novel processing of beta-amyloid precursor protein catalyzed by membrane type 1 matrix metalloproteinase releases a fragment lacking the inhibitor domain against gelatinase A. *Biochemistry (Mosc).* 2003; 42:6514–6526.
26. Ahmad M, et al. Cleavage of amyloid-beta precursor protein (APP) by membrane-type matrix metalloproteinases. *J Biochem.* 2006; 139:517–526. [PubMed: 16567416]

27. Scheltema RA, et al. The Q Exactive HF, a Benchtop mass spectrometer with a pre-filter, high-performance quadrupole and an ultra-high-field Orbitrap analyzer. *Mol Cell Proteomics*. 2014; 13:3698–3708. [PubMed: 25360005]
28. Folgueras AR, et al. Metalloproteinase MT5-MMP is an essential modulator of neuro-immune interactions in thermal pain stimulation. *Proc Natl Acad Sci U S A*. 2009; 106:16451–16456. [PubMed: 19805319]
29. Zhou Z, et al. Impaired endochondral ossification and angiogenesis in mice deficient in membrane-type matrix metalloproteinase I. *Proc Natl Acad Sci U S A*. 2000; 97:4052–4057. [PubMed: 10737763]
30. Shi Y, Kirwan P, Livesey FJ. Directed differentiation of human pluripotent stem cells to cerebral cortex neurons and neural networks. *Nat Protoc*. 2012; 7:1836–1846. [PubMed: 22976355]
31. Jacobsen H, et al. Combined treatment with a BACE inhibitor and anti-Abeta antibody gantenerumab enhances amyloid reduction in APPLondon mice. *J Neurosci*. 2014; 34:11621–11630. [PubMed: 25164658]
32. Moechars D, et al. Early phenotypic changes in transgenic mice that overexpress different mutants of amyloid precursor protein in brain. *J Biol Chem*. 1999; 274:6483–6492. [PubMed: 10037741]
33. Cai H, et al. BACE1 is the major beta-secretase for generation of Abeta peptides by neurons. *Nat Neurosci*. 2001; 4:233–234. [PubMed: 11224536]
34. Radde R, et al. A beta 42-driven cerebral amyloidosis in transgenic mice reveals early and robust pathology. *EMBO Rep*. 2006; 7:940–946. [PubMed: 16906128]
35. Nabavi S, et al. Engineering a memory with LTD and LTP. *Nature*. 2014; 511:348–352. [PubMed: 24896183]
36. Walsh DM, et al. Naturally secreted oligomers of amyloid beta protein potently inhibit hippocampal long-term potentiation in vivo. *Nature*. 2002; 416:535–539. [PubMed: 11932745]
37. Shankar GM, et al. Natural oligomers of the Alzheimer amyloid-beta protein induce reversible synapse loss by modulating an NMDA-type glutamate receptor-dependent signaling pathway. *J Neurosci*. 2007; 27:2866–2875. [PubMed: 17360908]
38. Shankar GM, et al. Amyloid-beta protein dimers isolated directly from Alzheimer's brains impair synaptic plasticity and memory. *Nat Med*. 2008; 14:837–842. [PubMed: 18568035]
39. Filser S, et al. Pharmacological Inhibition of BACE1 Impairs Synaptic Plasticity and Cognitive Functions. *Biol Psychiatry*. 2014
40. Busche MA, et al. Clusters of hyperactive neurons near amyloid plaques in a mouse model of Alzheimer's disease. *Science*. 2008; 321:1686–1689. [PubMed: 18802001]
41. Busche MA, et al. Critical role of soluble amyloid-beta for early hippocampal hyperactivity in a mouse model of Alzheimer's disease. *Proc Natl Acad Sci U S A*. 2012; 109:8740–8745. [PubMed: 22592800]
42. Hardy J, Selkoe DJ. The amyloid hypothesis of Alzheimer's disease: progress and problems on the road to therapeutics. *Science*. 2002; 297:353–356. [PubMed: 12130773]
43. Jonsson T, et al. A mutation in APP protects against Alzheimer's disease and age-related cognitive decline. *Nature*. 2012; 488:96–99. [PubMed: 22801501]
44. Kuhn PH, et al. Secretome protein enrichment identifies physiological BACE1 protease substrates in neurons. *EMBO J*. 2012; 31:3157–3168. [PubMed: 22728825]
45. Zhou L, et al. The neural cell adhesion molecules L1 and CHL1 are cleaved by BACE1 protease in vivo. *The Journal of biological chemistry*. 2012; 287:25927–25940. [PubMed: 22692213]
46. Blennow K, Zetterberg H, Haass C, Finucane T. Semagacestat's fall: where next for AD therapies? *Nat Med*. 2013; 19:1214–1215. [PubMed: 24100981]
47. Nolan RL, Teller JK. Diethylamine extraction of proteins and peptides isolated with a mono-phasic solution of phenol and guanidine isothiocyanate. *J Biochem Biophys Methods*. 2006; 68:127–131. [PubMed: 16750859]
48. Westmeyer GG, et al. Dimerization of beta-site beta-amyloid precursor protein-cleaving enzyme. *J Biol Chem*. 2004; 279:53205–53212. [PubMed: 15485862]

49. Fleck D, et al. Dual cleavage of neuregulin 1 type III by BACE1 and ADAM17 liberates its EGF-like domain and allows paracrine signaling. *J Neurosci.* 2013; 33:7856–7869. [PubMed: 23637177]
50. Jacobsen H, et al. Combined treatment with a BACE inhibitor and anti-Ab antibody gantenerumab enhances amyloid reduction in APPLondon mice. *J Neurosci.* 2014
51. Houeland G, et al. Transgenic mice with chronic NGF deprivation and Alzheimer's disease-like pathology display hippocampal region-specific impairments in short- and long-term plasticities. *J Neurosci.* 2010; 30:13089–13094. [PubMed: 20881126]
52. Townsend M, Shankar GM, Mehta T, Walsh DM, Selkoe DJ. Effects of secreted oligomers of amyloid beta-protein on hippocampal synaptic plasticity: a potent role for trimers. *J Physiol.* 2006; 572:477–492. [PubMed: 16469784]
53. Dombeck DA, Harvey CD, Tian L, Looger LL, Tank DW. Functional imaging of hippocampal place cells at cellular resolution during virtual navigation. *Nat Neurosci.* 2010; 13:1433–U1180. [PubMed: 20890294]
54. Mizrahi A, Crowley JC, Shtoyerman E, Katz LC. High-resolution in vivo imaging of hippocampal dendrites and spines. *J Neurosci.* 2004; 24:3147–3151. [PubMed: 15056694]
55. Grienberger C, Chen X, Konnerth A. NMDA receptor-dependent multidendrite Ca<sup>2+</sup> spikes required for hippocampal burst firing in vivo. *Neuron.* 2014; 81:1274–1281. [PubMed: 24560703]
56. Stosiek C, Garaschuk O, Holthoff K, Konnerth A. In vivo two-photon calcium imaging of neuronal networks. *Proc Natl Acad Sci U S A.* 2003; 100:7319–7324. [PubMed: 12777621]

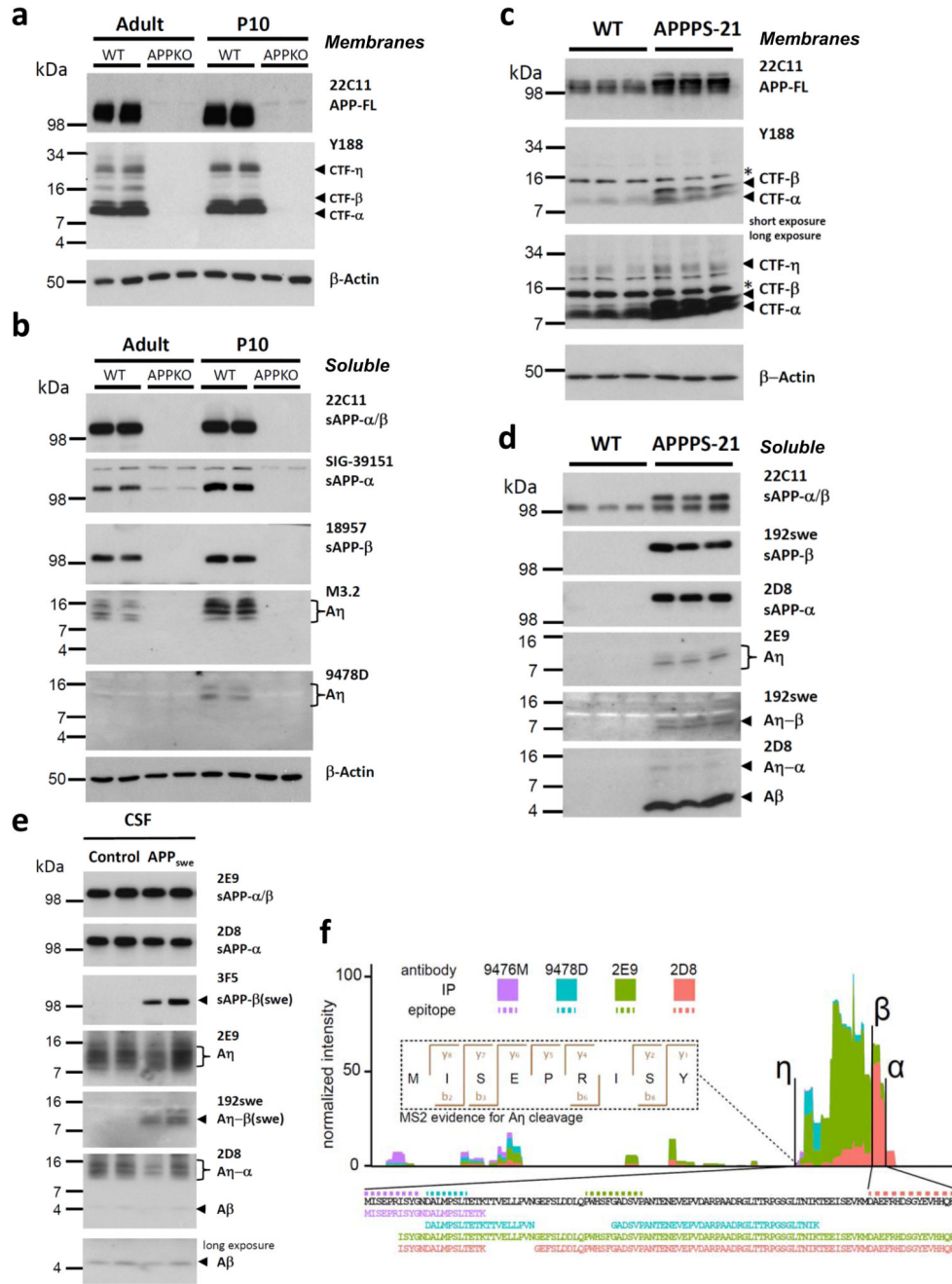


**Figure 1. A novel proteolytic processing pathway of APP.**

**a**, A 30 kDa N-terminally elongated APP-CTF- $\eta$  fragment is detected in membrane fractions obtained from brains of adult (22 month) and postnatal day 10 (P10) mice using antibody Y188 directed against the C-terminus of APP. CTF- $\eta$  is specifically found in young and old wild type (WT) mice but absent in APPKO19. In addition to this novel fragment, Y188 is detecting CTF- $\beta$  and CTF- $\alpha$ . Full-length APP (APP-FL) was detected with antibody 22C11.  $\beta$ -Actin served as loading control. **b**, A $\eta$  was identified as several closely spaced peptides detected in the soluble fraction of adult and P10 mice by antibody M3.2. A

similar pattern is detected by antibody 9478D that is specifically recognizing an N-terminal part of the A $\eta$  peptide (antibody 9478D may not be sensitive enough to detect the lower A $\eta$  levels in adult brain). sAPP- $\alpha$  and sAPP- $\beta$  are shown as additional controls. APPKO brains were used as controls for antibody specificities.  $\beta$ -Actin served as a loading control. **c**, Higher levels of CTF- $\eta$  are observed in RIPA lysates of APPPS1-21 mouse brains (long exposure) as compared to WT. Full-length APP (APP-FL) was detected with antibody 22C11.  $\beta$ -Actin served as a loading control. **d**, Soluble extracts of APPPS1-21 mouse brains contained A $\eta$  species detected by 2E9. A $\eta$ - $\beta$ (swe) was selectively detected by antibody 192swe in addition to sAPP- $\beta$ (swe). While 2D8 antibody detected robust levels of sAPP- $\alpha$ , only low levels of A $\eta$ - $\alpha$  could be detected in APPPS1-21 brain lysates due to the overexpression of APP<sup>swe</sup> transgene. **e**, A $\eta$  and A $\beta$  were readily detectable in 10  $\mu$ l of human CSF by antibody 2D8. Antibody 2E9 allowed the selective detection of A $\eta$  in the same samples, while 192swe specifically detected BACE1 cleaved A $\eta$ - $\beta$ (swe) in the mutation carriers, but not in controls. **f**, Mass spectrometry analysis of peptides isolated by immunoprecipitation with antibodies 2E9, 2D8, 9478D and 9476M (supplementary Fig. S3 a and b). Peptide intensities were summed per amino acid residue and plotted in relation to each other. We detected peptides from the complete A $\eta$ - $\alpha$  sequence (see also supplementary Fig. S3c). The fragmentation spectrum of the N-terminal A $\eta$  peptide (APP505-5013) shows good coverage of the b- and y-ion series and an Andromeda score of 88.5 [Doi [10.1021/Pr101065j](https://doi.org/10.1021/Pr101065j)].

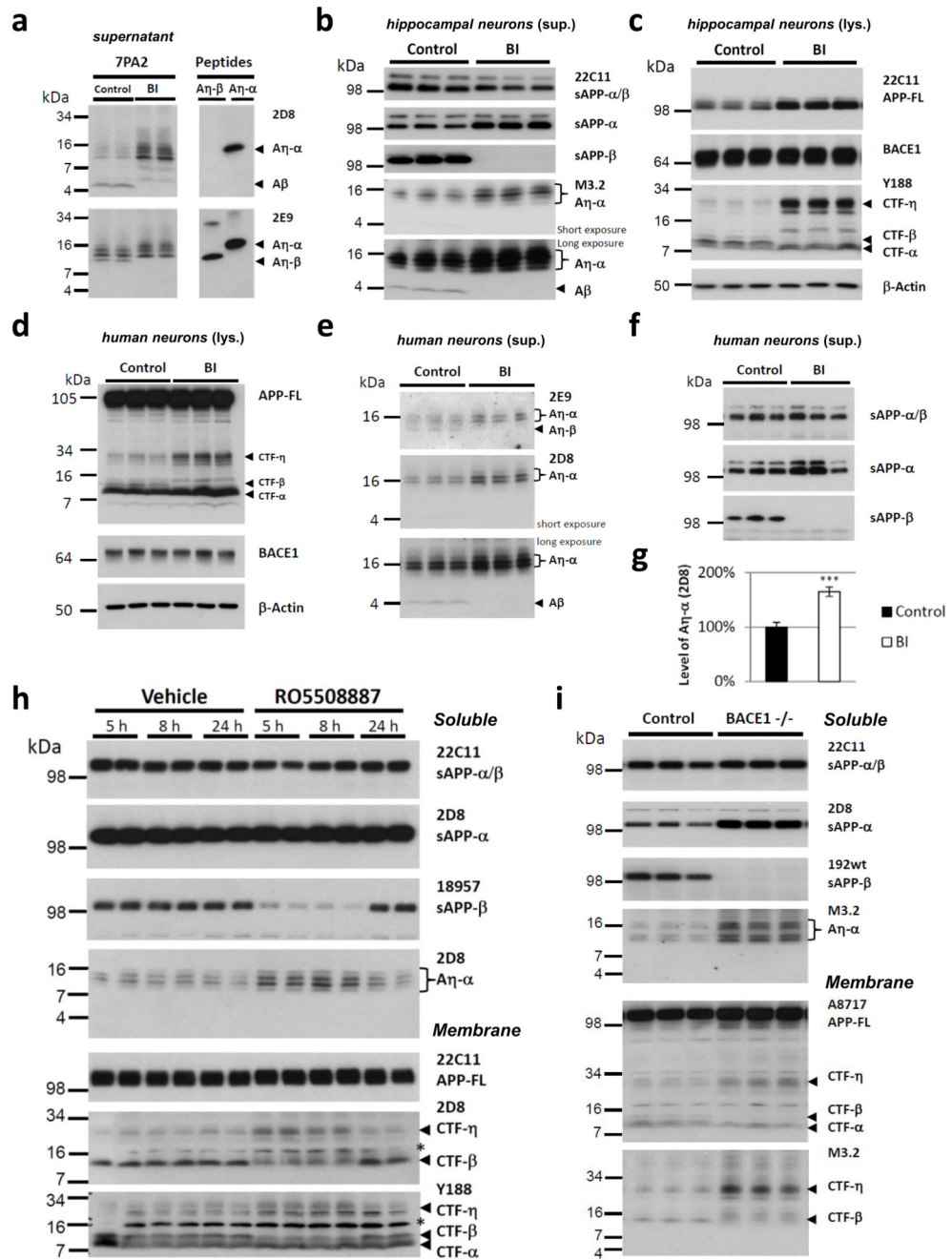


**Figure 2. Inhibition of BACE1 results in elevated levels of CTF-η and of Aη-α.**

**a**, Conditioned media of CHO cells expressing human APP<sub>V717F</sub> without or with BACE1 inhibition (BI; 2 μM Merck IV) were compared to synthetic peptides of Aη-β and Aη-α. Increased Aη-α peptide levels were observed upon BACE1 inhibitor treatment. The peptide with the lowest molecular weight, co-migrating with the synthetic peptide Aη-β, was diminished upon BACE1 inhibition. **b-c**, After overnight incubation without or with a BACE1 inhibitor (BI; 2 μM Merck IV), supernatants (sup.) (**b**) and lysates (lys.) (**c**) of DIV16 primary hippocampal neurons were analyzed by Western blotting. A strong increase of

endogenous A $\eta$ - $\alpha$  was observed upon BACE inhibition. **(b)**. Total levels of secreted APP (22C11) were unchanged while sAPP- $\alpha$  levels increased. The absence of sAPP- $\beta$  and A $\beta$  proves the effective blockade of BACE1 **(b)**. In cell lysates CTF- $\beta$  was undetectable when the BACE inhibitor was applied and CTF- $\eta$  was strongly increased **(c)**. While APP-FL levels were accumulating, CTF- $\alpha$  levels remained unchanged. BACE1 levels were similar in all samples.  $\beta$ -Actin served as loading control **(c)**. **d-g**, Similarly, human neurons differentiated from H9 embryonic stem cells<sup>30</sup> were incubated for 48 h with a BACE1 inhibitor (BI; 1  $\mu$ M LY2886721). **d**, In cell lysates enriched CTF- $\eta$  levels were detected, while CTF- $\beta$  levels were diminished. APP-FL and BACE1 levels were similar in all samples.  $\beta$ -Actin served as loading control. **e-g**, Supernatants were analyzed by Western blotting. While sAPP- $\beta$  levels dropped to undetectable levels upon BACE inhibition, A $\eta$ - $\alpha$  levels strongly increased as indicated by antibody 2D8 and 2E9 **(g)**, ImageG quantified intensities for 2D8 signal in **e**; 64,8% increase upon BACE1 inhibition, n=8; p < 0.001; Student's t-test). With antibody 2E9 we additionally detected a faster migrating band disappearing when BACE was blocked, demonstrating the selective reduction of A $\eta$ - $\beta$ . In supernatants of hippocampal neurons and of H9 induced neurons A $\beta$  could be detected only upon longer exposure, while for the detection of A $\eta$ - $\alpha$  much shorter exposures were sufficient. **h**, BACE1 inhibition *in vivo* resulted in enhanced production of A $\eta$ - $\alpha$  species in APP<sub>V717I</sub> mice. BACE1 inhibitor RO5508887 treated mice and vehicle treated controls were sacrificed and analyzed after 5, 8 or 24 h. BACE inhibition reduced sAPP- $\beta$  and CTF- $\beta$  and increased levels of A $\eta$ - $\alpha$  at 5 and 8 h after treatment. 24 h after the treatment these changes were normalized due to the clearance of the inhibitor. Background bands obtained with 2D8 and Y188 are indicated by asterisks. **i**, Western blot analysis of soluble extracts of P10 BACE1<sup>-/-</sup> mouse brains revealed a significant increase in A $\eta$ - $\alpha$  peptides as compared to controls. Total levels of secreted APP (22C11) were unchanged while sAPP- $\alpha$  levels increased. CTF- $\eta$  levels were increased in membrane lysates of the BACE1<sup>-/-</sup> mouse brain. As expected after an efficient BACE1 block, CTF- $\beta$  and sAPP- $\beta$  were severely reduced.

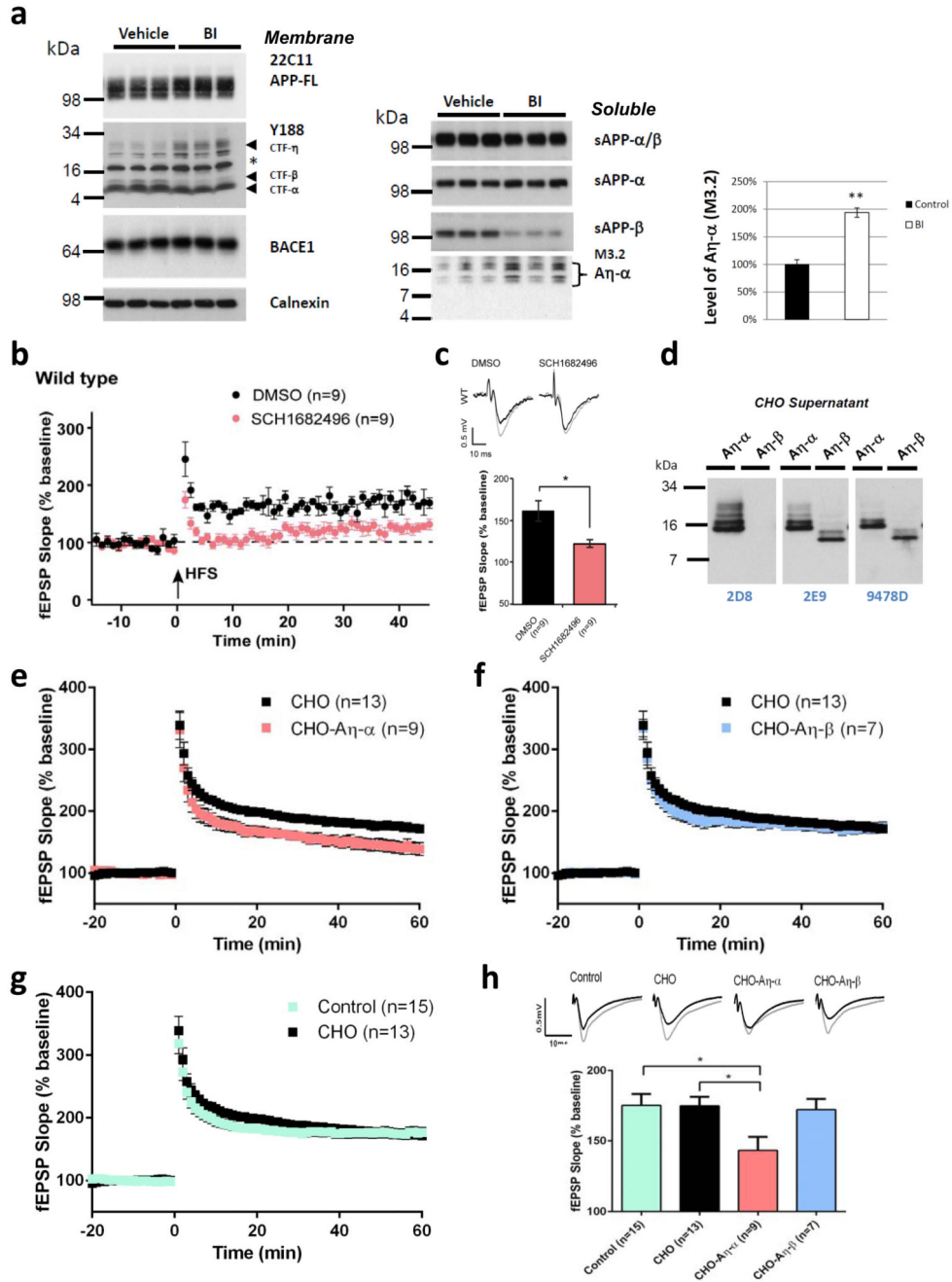


**Figure 3. Aη-α impairs hippocampal LTP.**

**a**, In membrane lysates of brains obtained from BACE inhibitor (BI, 100mg/kg SCH1682496) treated animals an increase in CTF-η was observed, which was paralleled by a strong reduction of CTF-β, while CTF-α was unchanged (left panel). APP-FL and BACE1 signals remained unchanged (asterisk indicates background band). Calnexin served as a loading control (Left panel). In the soluble fraction BACE inhibition resulted in enhanced production of Aη-α species which was detected by antibody M3.2 (right panel). Reduced sAPP-β levels indicated efficient BACE1 inhibition. revealed a 95,4% increase upon BACE1



inhibition,  $n=3$ ;  $p < 0.01$ , Student's  $t$ -test). **b-c**, Pharmacological inhibition of BACE lowers hippocampal LTP. Three hours after a single gavage of SCH1682496 (100 mg/kg) or vehicle, hippocampal slices were cut and baseline transmission and LTP measured. Note, that compared to vehicle treated controls in slices from inhibitor treated mice LTP was notably reduced. **c**, Representative fEPSPs recorded in CA1 area prior and 45 min after tetanization of Schaffer collaterals (top) with summary plots of the effects of the inhibitor and vehicle on fEPSP slopes in all examined groups. **d**, Soluble A $\eta$ - $\alpha$  and A $\eta$ - $\beta$  peptides were expressed in CHO cells. Conditioned media were analyzed with antibodies 2D8, 2E9 and 9478D for the presence of the larger A $\eta$ - $\alpha$  and the smaller A $\eta$ - $\beta$  peptides. **e-h**, SEC fractions containing A $\eta$  were diluted (1:15) in ACSF for the treatment of hippocampal slices and LTP measurements. A $\eta$ - $\alpha$  or A $\eta$ - $\beta$  and control SEC fractions (obtained from CHO cells transfected with the empty vector) were perfused over mouse hippocampal slices for 20 min after obtaining a stable baseline of a fEPSP at the CA3-CA1 synapse. After 20 minutes a high-frequency stimulation protocol was applied (HFS; 2x (100 Hz, 1 s) at 20 second inter-stimulus interval) to induce long-term potentiation (LTP). **e**, Supernatants from CHO cells expressing A $\eta$ - $\alpha$  significantly inhibited LTP; **f**, Supernatants from CHO cells expressing A $\eta$ - $\beta$  did not alter LTP. **g**, Supernatants from untransfected CHO cells did not alter LTP when compared to the control condition (ACSF only); **h**, summary graph of LTP magnitudes (as % of baseline) calculated 45-60 minutes post-HFS from graphs in e-g with statistical analysis ( $*p < 0.05$ ); error bars represent s.e.m.  $n$  = number of fields. For each condition, sample fEPSP traces pre-LTP (black) and 45-60 min post-LTP (grey) induction are shown.

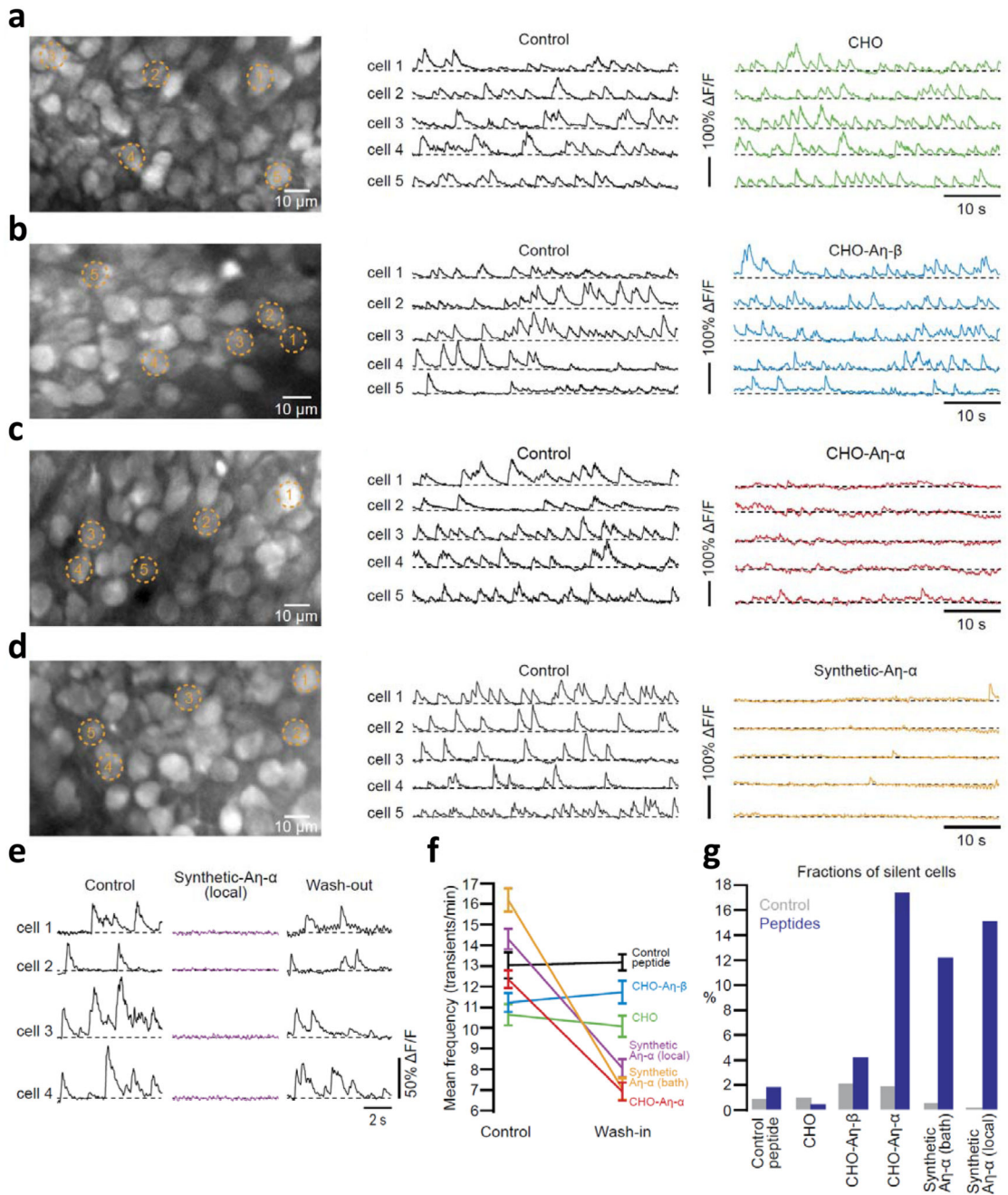


**Figure 4. Aη-α reduces neuronal activity *in vivo*.**

**a-d** (left panels), *In vivo* two-photon images of CA1 hippocampal neurons labeled with the fluorescent calcium indicator fluo-8 AM. (middle and right panels), Calcium transients of 5 representative neurons, marked in the corresponding left panels a-d, before and during bath-application of Aη peptides (panels b-d) and CHO conditioned media (panel a). **e**, Calcium transients in hippocampal neurons before, during and after local application of synthetic Aη-α. **f**, Summary results of the changes in the average rates of calcium transients (error bars represent s.e.m;  $p < 0.001$  for CHO-Aη-α ( $12.36 \text{ transients/min} \pm 0.43$  vs.  $6.91 \pm 0.44$ ,  $n =$

206 cells in three mice), bath-applied synthetic A $\eta$ - $\alpha$  ( $16.19 \pm 0.56$  vs.  $7.06 \pm 0.53$ , n = 163 cells in three mice) and locally applied A $\eta$ - $\alpha$  ( $14.30 \pm 0.5$  vs.  $8.05 \pm 0.44$ , n = 198 cells in four mice);  $p > 0.05$  for CHO ( $10.65 \pm 0.51$  vs.  $10.09 \pm 0.52$ , n = 188 cells in three mice), control peptide ( $12.62 \pm 0.44$  vs.  $13.17 \pm 0.40$ , n = 212 cells in three mice) and CHO-A $\eta$ - $\beta$  ( $11.23 \pm 0.46$  vs.  $11.72 \pm 0.55$ , n = 186 cells in three mice); Students T-test). **g**, Summary results, displayed as bar graphs, of the changes in the fractions of silent neurons ( $p < 0.001$  for CHO-A $\eta$ - $\alpha$  (1.94 % vs. 17.48), bath-applied synthetic A $\eta$ - $\alpha$  (0.62 vs. 12.27), locally applied A $\eta$ - $\alpha$  (0 vs. 15.15);  $p > 0.05$  for CHO (1.06 vs. 0.53), control peptide (0.94 vs. 1.90) and CHO-A $\eta$ - $\beta$  (2.15 vs. 4.30); Fisher's exact test)